

1 Rapid antimicrobial sensitivity testing by single cell 2 nanoscale optical interference

3

4 Isabel Bennett^{1,2}, Alice Pyne^{1*}, Rachel McKendry^{1,2*}

5 ¹London Centre for Nanotechnology, University College London, 17-19 Gordon Street, London, WC1H 0AH
6 UK

7 ²Division of Medicine, University College London, Cruciform Building, Gower Street, London, WC1E 6BT UK

8

9 *Corresponding authors: r.a.mckendry@ucl.ac.uk; alice.pyne@ucl.ac.uk

10 Abstract

11 Growing antimicrobial resistance (AMR) is a serious global threat to human health, with
12 estimates of AMR leading to 10 million deaths per year and costing the global economy
13 \$100tn by 2050^{1,2}. Current methods to detect resistance include phenotypic antibiotic
14 sensitivity testing (AST) which measures bacterial growth and is therefore hampered by slow
15 time to result (~12-24 hours). Therefore new rapid phenotypic methods for AST are urgently
16 needed³. Here we describe a novel method for detecting phenotypic antibiotic resistance in
17 ~45 minutes, capable of detecting single bacteria. The method uses a sensitive laser and
18 detector system to measure nanoscale optical interference of single bacterial cells present in
19 media, with simple sample preparation. This provides a read out of bacterial antibiotic
20 resistance by detecting growth (resistant) or death (sensitive), much faster than current
21 methods. We demonstrate the potential of this technique by determining resistance in both
22 lab and clinical strains of *E. coli*, a key species for clinically burdensome urinary tract
23 infections. This work provides the basis for a simple and fast diagnostic tool to detect
24 antibiotic resistance in bacteria, reducing the health and economic burdens of AMR.

25

26 Main

27 Antimicrobial resistance (AMR) is steadily increasing and poses a major threat to global
28 health. The increase in AMR has been caused by several factors including the overuse of
29 antibiotics⁴. Despite the growth of AMR, methods for antibiotic susceptibility testing (AST)
30 have remained relatively unchanged for several decades. In common AST methods bacterial
31 growth is used as a measure of sensitivity to antibiotics, determined directly by an increase in

32 media turbidity (the number of bacteria) or indirectly by the release of fluorescent
33 metabolites. These phenotypic methods provide *in vitro* confirmation of resistances in
34 isolated bacterial species, which are inferred from known resistance genes in genetic
35 methods. However phenotypic methods are inherently limited by the speed of bacterial
36 growth (for example, the doubling time of *E. coli* is 20 minutes, whereas *M. tuberculosis* is
37 15-12 hours), meaning these methods require long culture times (12-24 hours, or longer for
38 some species) for an observable change to occur. These delays result in empirical prescribing
39 of antibiotics for patients instead of targeted treatment, which has been shown to increase
40 mortality from sepsis fivefold⁵, in addition to being a driver of resistance. Having access to
41 the identity and antibiogram of the pathogen just a few hours earlier could avoid unnecessary
42 costs associated with inappropriate prescribing, increase patient welfare, and reduce the
43 effects of AMR^{6,7}. Therefore to reduce the damaging effects of AMR, we require solutions in
44 the form of novel diagnostic tools to detect resistance and improve antibiotic stewardship,
45 surveillance and patient management⁸.

46

47 Recent developments in this field have exploited single cell methods for faster and more
48 sensitive detection of antibiotic resistance. This has been achieved by miniaturising the
49 volume observed using microfluidics⁹⁻¹¹, measuring mass or mechanical changes¹¹⁻¹⁴, or by
50 exploiting machine learning techniques for video tracking analysis of single cells¹⁵⁻¹⁷. Despite
51 advances in the detection limit, and speed of testing, these are mostly complex set-ups, which
52 remain far from point of care.

53

54 Here we report a novel optical method for rapid detection of antibiotic resistance in bacterial
55 solutions with single cell resolution. This method uses a laser and sensitive photodetector to
56 measure the effect of antibiotics on bacterial growth, as briefly described here. A reflective
57 surface (small cantilever) is immersed in filtered growth media, off which a laser is reflected
58 onto a photodiode detector (Figure 1a). In media without bacteria we observe no movement
59 in the laser (Figure 1b). On inoculation with bacteria, bacteria free in the growth media move
60 through the path of the laser. This movement interferes with the laser beam, causing it to shift
61 on the detector, observable as peaks in the signal (Figure 1c). On addition of antibiotic to the
62 media, cell death occurs in sensitive bacteria, and fewer bacteria are detected passing through
63 the laser. This results in a decrease in the number of peaks after ~45 minutes (Figure 1d).

64

65 To determine the origin of the peaks in the signal, we reduced the bacterial concentration
66 level to $\sim 10^5$ CFU (colony forming units, a standard measure of bacterial concentration). At
67 this concentration individual peaks within the signal can be observed (Figure 2a). When a
68 single bacterium is tracked optically crossing the path of the laser (Figure 2b, blue circle), a
69 corresponding peak in the signal can be observed in the data (Figure 2c). These peaks are of
70 varying width and amplitude, due to differing angle and distance at which the bacteria pass
71 through the laser. As more bacteria are added to the system (i.e. increasing CFU), the number
72 of peaks in the signal also increases (Figure 2d), indicating that it is the bacteria giving rise to
73 the signal.

74

75 We have shown that we can link the number of peaks observed to the number of viable
76 bacteria in solution, which we can exploit to determine antibiotic resistance. If we determine
77 the number of peaks (or bacterial crossings) at distinct time points during an experiment (for
78 example ‘media only’ (blue box), ‘inoculated media’ (green box), ‘inoculated media
79 containing antibiotic’ (red box)) (SI Figure 1), we can see a distinct pattern where bacterial
80 crossings increase on addition of bacteria to the system (Figure 3a, at blue dotted line), and
81 decrease around 45 minutes (about two replication cycles for *E. coli*) after the addition of
82 antibiotic (yellow dotted line) in the case of sensitive strain. This pattern is not observed in a
83 control with solution added containing no antibiotic (SI Figure 2). To note is that the two
84 peaks observed in the signal which correspond to the addition of bacteria and antibiotic
85 (Figure 3a, blue and yellow dotted lines, respectively) occur due to mixing of the system.
86 These peaks settle to a baseline and are observed in control experiments (SI Figure 2, points
87 ‘3’ and ‘4’).

88

89 Using this method we can differentiate sensitive and resistant strains of *E. coli*. As described
90 above, we observe a reduction in signal after addition of antibiotic for sensitive strains
91 (Figure 3a, green); for resistant strains, there is an increase in signal (Figure 3a, red). Though
92 the trend remains the same, the magnitude of the signal change can vary (SI Figure 3a) based
93 on multiple factors which effect growth rates, including inoculant concentration, strain, and
94 temperature, for example. We therefore normalise the data to the baseline before the addition
95 of antibiotic when comparing between experiments (S_{baseline}) (SI Figure 3b).

96

97 To obtain a systematic readout of antibiotic sensitivity across experiments, including multiple
98 strains and antibiotics, we obtain a normalised measure of bacterial growth as follows. We

99 define antibiotic sensitivity as $r_{\text{sensitivity}}$: the ratio of S_{baseline} and 45 minutes post-antibiotic
100 treatment ($S_{\text{antibiotic}}$), shaded blue in Figure 3a. $r_{\text{sensitivity}}$ provides a binary readout of
101 sensitivity, $r_{\text{sensitivity}} \leq 1$ indicates cell death or inhibition of bacterial growth, and sensitivity to
102 the antibiotic in solution; $r_{\text{sensitivity}} > 1$ indicates bacterial growth, and therefore resistance to
103 the antibiotic used. This method allows for both bactericidal and bacteriostatic antibiotics to
104 be used, as $r_{\text{sensitivity}} < 1$ indicates a decrease in cell number, or cell death (bactericidal);
105 $r_{\text{sensitivity}} = 1$ would indicate inhibition of growth, but little cell death (bacteriostatic). For
106 Figure 3a with ampicillin, $r_{\text{sensitivity}} = 0.5$ for the green strain (sensitive) and $r_{\text{sensitivity}} = 1.1$ for
107 the red strain (resistant). For kanamycin, $r_{\text{sensitivity}} = 0.92$ for a sensitive strain and $r_{\text{sensitivity}} =$
108 2.0 for a resistant strain (green and red, respectively SI Figure 4).

109

110 Having shown that we can use $r_{\text{sensitivity}}$ as a measure of bacterial sensitivity, we now apply
111 this method to a range of concentrations of ampicillin to determine the minimum inhibitory
112 concentration (MIC) for the *E.coli* strain BL21 (Figure 3b). The MIC value is defined as the
113 lowest concentration of an antibiotic that will inhibit the visible growth of a bacterial strain¹⁸,
114 and is used to inform clinical breakpoints and provide patient-dose information for
115 prescribing treatment. At low ampicillin concentrations (0-12.5 $\mu\text{g/mL}$) $r_{\text{sensitivity}} > 1$, however
116 at increased ampicillin concentrations (50-125 $\mu\text{g/mL}$) $r_{\text{sensitivity}} < 1$. This indicates an MIC of
117 12.5-50 $\mu\text{g/mL}$ ampicillin for this strain. This result is within the range determined by broth
118 microdilution, the gold standard method (8-16 $\mu\text{g/mL}$). Despite difficulties in variability of
119 measuring MICs^{19,20}, these values are used by clinicians when making decisions about patient
120 care (antibiotic selection and dosing), and hence are an important result for any new
121 diagnostic tool to accurately measure.

122

123 Uropathogenic *E. coli* (UPEC) is the leading cause of urinary tract infections (UTIs)²¹, and is
124 clinically burdensome across the globe. AMR has increased in UTIs and hence represents an
125 excellent clinical target for a new diagnostic tool. Here we demonstrate potential for the
126 optical interference method by testing on an *E. coli* clinical isolate. As shown in Figure 3c,
127 treatment of the clinical isolate with 125 $\mu\text{g/mL}$ ampicillin and trimethoprim resulted in no
128 decrease in signal, and gave $r_{\text{sensitivity}} > 1$ within 45 minutes (Figure 3d). This was confirmed
129 by broth microdilution (resistance $>256 \mu\text{g/mL}$ ampicillin and trimethoprim). These detected
130 resistances were in agreement with the resistance spectrum obtained from the hospital (Great
131 Ormond Street Hospital, London) measured by the gold standard method in the clinical
132 laboratory (SI Table 1). This study demonstrates the ability of this method to successfully

133 carry out an AST for a strain of bacteria isolated from a patient within 45 minutes of the
134 addition of antibiotic.

135

136 To conclude, in the face of AMR novel rapid methods to detect resistance in bacteria are
137 needed to prevent its further spread and development. We have shown that our novel optical
138 interference method can rapidly differentiate between resistant and sensitive phenotypes in
139 lab and clinical strains of *E. coli* and determine MIC values to the same range as current gold
140 standard methods. We obtain a read out of bacterial sensitivity within ~45 minutes of the
141 addition of antibiotic. This method lends itself to miniaturisation and automation, requiring a
142 stable reflective surface which could be embedded within a 96-well plate for automated
143 reading, with a laser and photodetector readout. This method can be exploited as a new rapid
144 phenotypic method for AST, to provide these time-critical results to inform patient care and
145 antibiotic stewardship.

146 Methods

147

148 Experimental method:

149 A stiff AC160 TS cantilever ($k = 26$ N/m; Olympus, Japan) was loaded onto an AFM head
150 (JPK Nanowizard 3 ULTRA Speed; JPK Instruments, Germany) and immersed in filtered
151 Luria Broth (LB; Sigma-Aldrich, USA) in a 35 mm diameter glass bottom petri dish (WillCo
152 Wells, Netherlands). The cantilever spring constant was calibrated using the thermal noise
153 method in the JPK software to convert vertical deflection from volts to nm. The cantilever
154 was allowed to equilibrate for 15 minutes, during which time vertical deflection of the laser
155 was measured. The LB media was then inoculated with bacteria to a constant concentration
156 ($\sim 10^5$ CFU) and recording was started again for another 40 minutes to obtain pre-antibiotic
157 baseline. Antibiotic solution was then added to directly to the LB + bacteria solution to a
158 desired final concentration, and deflection recording was then measured.

159

160 During experiments only the real-time scan function was used to monitor vertical deflection
161 of the laser. Experiments were conducted at 28°C in an acoustic isolation hood. Prior to the
162 start of the experiments, the AFM laser was left on for ~2 hours to ensure the laser had
163 warmed up fully and to reduce laser power fluctuations which would affect the drift of the
164 signal.

165

166 Reagents:

167 Luria broth (LB) and antibiotics (ampicillin, kanamycin, trimethoprim) were all supplied by
168 Sigma-Aldrich (USA).

169

170 Bacterial Strains:

171 *E. coli* BL21(DE3)pLysS competent cells (Promega, UK) were selected for their suitability
172 for transformation with a plasmid containing ampicillin resistance (pRSET/EmGFP plasmid;
173 Invitrogen, UK).

174

175 A clinical isolate of *E. coli* was obtained from the microbiology repository of Great Ormond
176 Street Hospital (London, UK).

177

178 Bacterial preparation:

179 An LB media (Sigma-Aldrich) plate was streaked with BL21 *E. coli* (Promega) or clinical
180 isolate *E. coli* (obtained from Great Ormond Street Hospital) from frozen stocks in a sterile
181 hood. These were grown up overnight at 37°C. A single colony was used to inoculate 4 mL
182 LB media, which was incubated at 37°C for 2 hours (225 r.p.m. shaking), to obtain mid-log
183 phase growth. The OD₆₀₀ of the culture was measured using a Nanodrop One-C (Thermo
184 Scientific), and a final OD₆₀₀ for bacterial inoculation for experimental measurement was
185 adjusted to keep as constant as possible.

186

187 Bacterial transformation with ampicillin resistance:

188 An aliquot of competent bacterial stock was thawed on ice for 20-30 minutes. 1-5 μ L (10pg-
189 100ng) pRSET-EmGFP plasmid (Invitrogen, CA, USA) was mixed with 25 μ L thawed
190 bacterial solution and incubated for 5-10 minutes on ice, followed by heat shock treatment at
191 42°C for 40 seconds and returned to ice for two further minutes. 500 μ L warmed SOC media
192 was added, and this was incubated at 37°C at 225 r.p.m. for one hour. 50 μ L was plated onto
193 an agar plate which contained 50 μ g/mL nafcillin/ampicillin mixture. This plate was
194 incubated overnight at 37°C and colonies used were made into frozen stocks for experimental
195 use.

196

197 Data analysis:

198 Vertical deflection data (nm) was recorded on JPK Nanowizard 3 software at 20 kHz
199 sampling frequency. This raw data (SI Figure 5a) was then processed in 800 second “chunks”

200 using analysis code written in Matlab. This code applies a Savitzky-Golay finite impulse
201 response (FIR) smoothing filter of polynomial order 2 to the data, with a filtering frequency
202 of 101 Hz (SI Figure 5b). A Savitzky-Golay smoothing filter was chosen as this function can
203 filter noisy data effectively without removing high frequency data.

204

205 To identify the number of bacterial crossings, both local maxima and minima were identified,
206 as bacteria moving through the laser was observed to cause both peaks and dips in the signal
207 (SI Figure 5c, peaks labelled with blue triangles). A “Peak Finder” function was used to
208 identify local minima/maxima in the signal, where a “peak” was defined as having a
209 threshold drop of at least 0.5 nm on each side. This was to ensure that only the larger peaks
210 were counted, which correspond to bacteria moving across the laser. Smaller “noise” seen in
211 the signal was not attributed to actual bacterial crossings, but could be due to partial
212 crossings, or a change of orientation of bacteria within the laser during a crossing. This
213 threshold peak prominence value of 0.5 nm was applied empirically across all files when
214 carrying out the analysis to remove any bias of identifying peaks in the signal.

215

216 Across the experiment, the number of peaks was calculated for a subsampled time frame to
217 increase the resolution of the data from 800 seconds to 267 seconds, and plotted across the
218 experimental conditions of LB media, addition of bacteria, addition of antibiotic (SI Figure
219 5d).

220

221 To calculate the antibiotic sensitivity ($r_{\text{sensitivity}}$) the ratio of the signal pre-antibiotic addition,
222 S_{baseline} , and 45 minutes post-antibiotic addition, $S_{\text{antibiotic}}$ (SI Figure 5d). $r_{\text{sensitivity}}$ provides a
223 binary readout of sensitivity, $r_{\text{sensitivity}} \leq 1$ indicates cell death or inhibition of bacterial
224 growth, and sensitivity to the antibiotic in solution; $r_{\text{sensitivity}} > 1$ indicates bacterial growth,
225 and therefore resistance to the antibiotic used.

226

227 Acknowledgements

228 This work was supported by i-sense EPSRC IRC in Early Warning Sensing Systems in
229 Infectious Disease (EP/K031953/1), ERC AntiMicroResist grant (xxxx), i-sense EPSRC IRC
230 in Agile Early Warning Sensing Systems for Infectious Diseases and Antimicrobial
231 Resistance (EP/R00529X/1), EPSRC Royal Society Wolfson Research Merit Award, and by
232 UKRI/ MRC Rutherford Innovation Fellowship (MR/R024871/1). I.B. funded by EPSRC
233 UCL Impact Award Grant. The authors would like to thank E. Gray for microbiology
234 knowledge, K. Harris and R. Doyle for providing the clinical isolate, and T. Evans and B.
235 Miller for assistance with data analysis.

236

237 **Author Contributions**

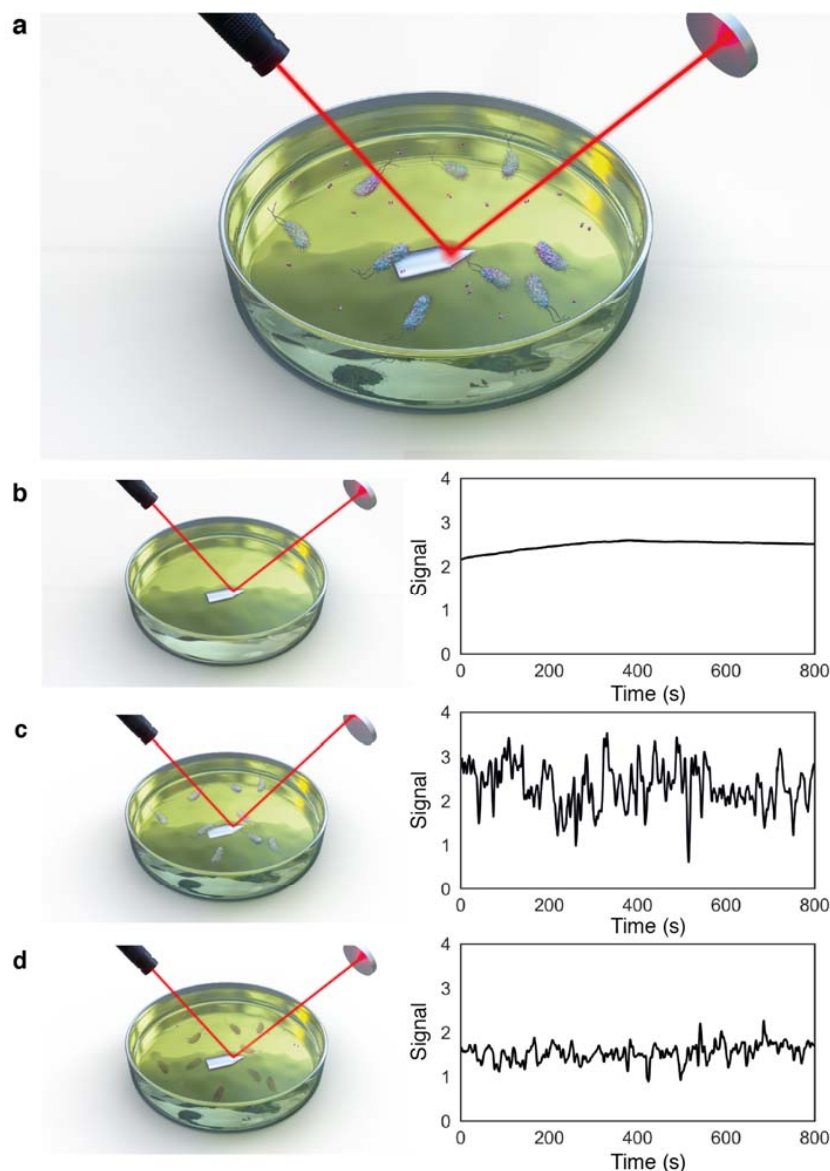
238 I.B., A.L.B.P. and R.M.K. designed the study. I.B. performed the optical interference
239 experiments. I.B. and A.L.B.P. analysed the data. I.B. and A.L.B.P. wrote the paper. All
240 authors discussed the results and commented on the manuscript.

241

242 **Competing Interests**

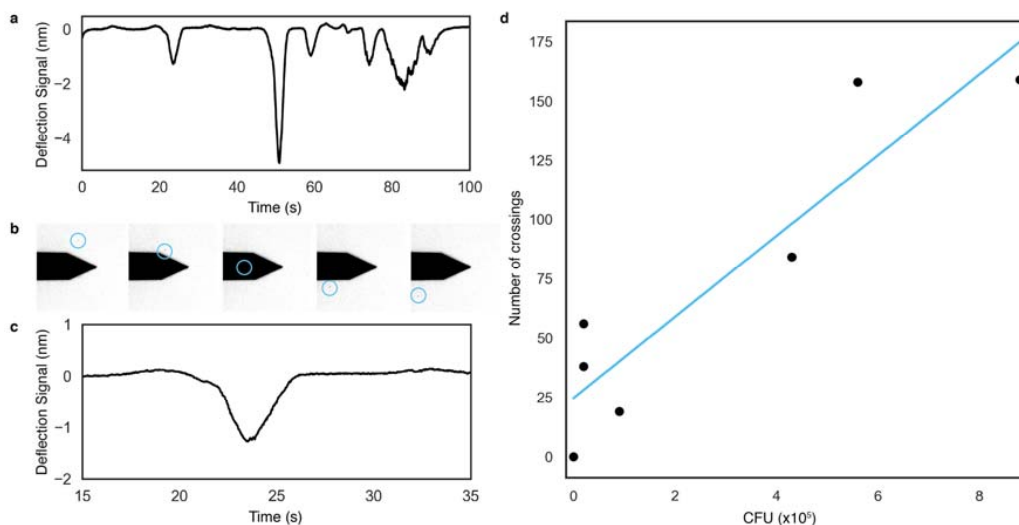
243 The authors declare no competing financial interests.

244 **Figures**



245

246 **Figure 1. Principles of nanoscale optical interference method.** a, Illustration of bacterial
247 cells inoculated in growth media with antibiotic molecules, with laser reflecting off cantilever
248 surface onto photodiode detector. Bacteria in solution move into the laser beam, which
249 interfere and cause the laser to move on the detector. This results in peaks in the measured
250 signal. Photodiode signal measured in media solution without bacterial inoculant (b), with
251 bacteria in solution (c) and 45 mins after addition of antibiotic (d). Signal decreases after
252 addition of antibiotic for sensitive strains.



253

254 **Figure 2. Signal caused by single bacteria decreases after 45 minutes from antibiotic**
255 **addition. a**, At low bacterial inoculant concentration, individual peaks can be identified
256 within the signal. Combined optical tracking and signal measurement shows movement of
257 single bacterium (blue circle) through laser path (**b**, optical images) as a single peak in the
258 signal (**c**). **d**, Effect of bacterial concentration (CFU, $\times 10^5$) on number of bacterial
259 crossings.

260

261

262

263

264

265

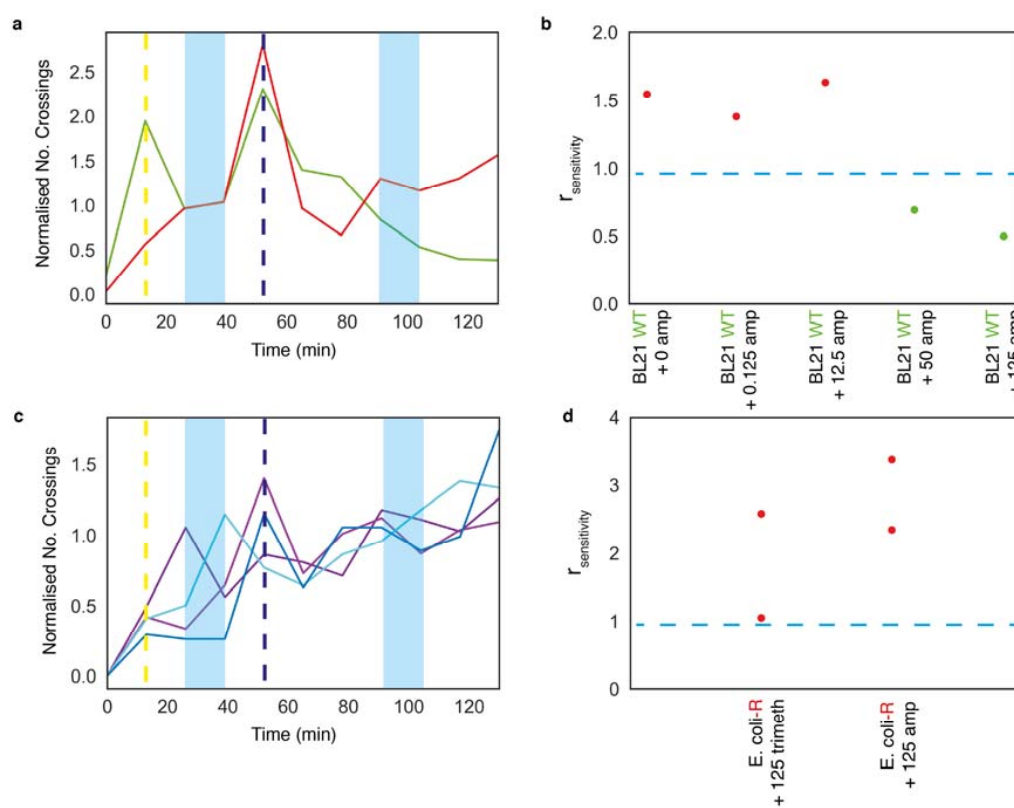
266

267

268

269

270



271

272 **Figure 3. Systematic analysis of susceptibility in clinical and laboratory strains of *E.***

273 *coli*. **a**, Susceptibility of BL21-WT (S, green) and BL21-ampR *E. coli* (R, red) to 125 µg/mL

274 ampicillin. Addition of bacteria (yellow dotted line) and antibiotic solution (dark blue dotted

275 line) to the system cause large fluctuations in the signal as the liquid is mixed, which

276 dissipate within ~800 seconds. Number of bacterial crossings in a given time period, here 800

277 seconds, is plotted. The number of bacterial crossings shows a decrease 45 minutes after

278 antibiotic addition. **b**, Determination of resistance profile, with sensitivity readout ($r_{\text{sensitivity}}$).

279 $r_{\text{sensitivity}}$ was calculated using the ratio of crossings post-antibiotic and pre-antibiotic at set

280 time points marked in blue in **a**. Strains were determined to be sensitive (S) if $r_{\text{sensitivity}} < 1$

281 (green); or resistant (R) if $r_{\text{sensitivity}} \geq 1$ (red), cut off ($r_{\text{sensitivity}} = 1$) shown as blue dashed line.

282 Shown for five concentrations of ampicillin and BL21 *E. coli* **c**, Susceptibility of a clinical

283 isolate of *E. coli*, determined to be resistant to both ampicillin (purple lines) and trimethoprim

284 (blue lines). **d**, Determination of resistance profile. $r_{\text{sensitivity}}$ for repeats of clinical isolate with

285 125 µg/mL trimethoprim and ampicillin. Antibiotic concentrations are given in µg/mL.

286

287

288

References

- 1 The Review on Antimicrobial Resistance Chaired by Jim O'Neill. Antimicrobial Resistance: Tackling a Crisis for the Future Health and Wealth of Nations. (2014).
- 2 Health, D. o. Annual Report of the Chief Medical Officer: Volume Two Infections and the rise of antimicrobialresistance. (2011).
- 3 Doern, C. D. The Slow March toward Rapid Phenotypic Antimicrobial Susceptibility Testing: Are We There Yet? *J Clin Microbiol* **56**, doi:10.1128/JCM.01999-17 (2018).
- 4 Chatterjee, A. *et al.* Quantifying drivers of antibiotic resistance in humans: a systematic review. *Lancet Infect Dis* **18**, e368-e378, doi:10.1016/S1473-3099(18)30296-2 (2018).
- 5 Kumar, A. *et al.* Initiation of inappropriate antimicrobial therapy results in a fivefold reduction of survival in human septic shock. *Chest* **136**, 1237-1248, doi:10.1378/chest.09-0087 (2009).
- 6 Doern, G. V., Vautour, R., Gaudet, M. & Levy, B. Clinical impact of rapid in vitro susceptibility testing and bacterial identification. *J Clin Microbiol* **32**, 1757-1762 (1994).
- 7 Barenfanger, J., Drake, C. & Kacich, G. Clinical and financial benefits of rapid bacterial identification and antimicrobial susceptibility testing. *Journal of Clinical Microbiology* **37**, 1415-1418 (1999).
- 8 The Review on Antimicrobial Resistance Chaired by Jim O'Neill. Tackling Drug-Resistant Infections Globally: Final Report and Recommendations. (2016).
- 9 Pitruzzello, G. *et al.* Multiparameter antibiotic resistance detection based on hydrodynamic trapping of individual E. coli. *Lab Chip* **19**, 1417-1426, doi:10.1039/c8lc01397g (2019).
- 10 Boedicker, J. Q., Li, L., Kline, T. R. & Ismagilov, R. F. Detecting bacteria and determining their susceptibility to antibiotics by stochastic confinement in nanoliter droplets using plug-based microfluidics. *Lab on a Chip - Miniaturisation for Chemistry and Biology* **8**, 1265-1272, doi:10.1039/b804911d (2008).
- 11 Etayash, H., Khan, M. F., Kaur, K. & Thundat, T. Microfluidic cantilever detects bacteria and measures their susceptibility to antibiotics in small confined volumes. *Nature Communications* **7**, 12947, doi:10.1038/ncomms12947 (2016).
- 12 Longo, G. *et al.* Rapid detection of bacterial resistance to antibiotics using AFM cantilevers as nanomechanical sensors. *Nat Nanotechnol* **8**, 522-526, doi:10.1038/nnano.2013.120 (2013).
- 13 Bermingham, C. R. *et al.* Imaging of sub-cellular fluctuations provides a rapid way to observe bacterial viability and response to antibiotics. *bioRxiv*, 460139, doi:10.1101/460139 (2018).
- 14 Ramos, D. *et al.* Detection of bacteria based on the thermomechanical noise of a nanomechanical resonator: origin of the response and detection limits. *Nanotechnology* **19**, 035503, doi:10.1088/0957-4484/19/03/035503 (2008).
- 15 Choi, J. *et al.* A rapid antimicrobial susceptibility test based on single-cell morphological analysis. *Science Translational Medicine* **6**, doi:10.1126/scitranslmed.3009650 (2014).
- 16 Syal, K. *et al.* Antimicrobial Susceptibility Test with Plasmonic Imaging and Tracking of Single Bacterial Motions on Nanometer Scale. *ACS Nano* **10**, 845-852, doi:10.1021/acsnano.5b05944 (2016).
- 17 Yu, H. *et al.* Phenotypic Antimicrobial Susceptibility Testing with Deep Learning Video Microscopy. *Anal Chem* **90**, 6314-6322, doi:10.1021/acs.analchem.8b01128 (2018).

- 18 Andrews, J. M. Determination of minimum inhibitory concentrations. *Journal of Antimicrobial Chemotherapy* **48**, 5-16 (2001).
- 19 Annis, D. H. & Craig, B. A. The effect of interlaboratory variability on antimicrobial susceptibility determination. *Diagn Microbiol Infect Dis* **53**, 61-64, doi:10.1016/j.diagmicrobio.2005.03.012 (2005).
- 20 Mouton, J. W., Meletiadis, J., Voss, A. & Turnidge, J. Variation of MIC measurements: the contribution of strain and laboratory variability to measurement precision. *J Antimicrob Chemother* **73**, 2374-2379, doi:10.1093/jac/dky232 (2018).
- 21 Flores-Mireles, A. L., Walker, J. N., Caparon, M. & Hultgren, S. J. Urinary tract infections: epidemiology, mechanisms of infection and treatment options. *Nat Rev Microbiol* **13**, 269-284, doi:10.1038/nrmicro3432 (2015).